

of the  $\text{CN}^-$  adducts of myeloperoxidase, horseradish peroxidase,<sup>46</sup> and sulfite reductase.<sup>15j</sup> We wish to point out that a bent FeCN structure will lead to an observed downshift of  $\nu(\text{Fe-CN})$  mode for the cyanide adducts of sterically hindered hemes.<sup>47</sup>

#### Summary

The resonance Raman spectra of the nitric oxide adducts of cytochrome P450cam in several substrate-bound forms are re-

(46) Lopez-Garriga, J. J.; Oertling, W. A.; Kean, R. T.; Hoogland, H.; Wever, R.; Babcock, G. T. *Biochemistry* 1990, 29, 9387-9395.

(47) Tanaka, T.; Yu, N.-T.; Chang, C. K. *Biophys. J.* 1987, 52, 801-805.

(48) Tsubaki, M.; Srivastava, R. B.; Yu, N.-T. *Biochemistry* 1982, 1132.

ported. These adducts are formulated as six-coordinate, low-spin compounds. The  $\nu(\text{Fe-NO})$  and  $\delta(\text{Fe-NO})$  modes are detected and assigned through isotopic substitution and found to be dramatically lower than those of the corresponding myoglobin and horseradish peroxidase adducts. On the basis of a consideration of both electronic and kinematic factors, the effect of the substrate structure on the metal-ligand vibrations can be explained by adopting a slightly bent geometry of the intrinsically linear Fe-NO linkage in the substrate-bound form.

**Acknowledgment.** This work was supported by a grant from the National Institute of Health (DK35153 to J.R.K.).

## Investigation of the Kinetic Window for Generation of $^{13}\text{C}$ $\text{T}_0$ -S CIDNP Derived from Long-Chain Biradicals by Tuning the Rates of Bimolecular Scavenging and Intersystem Crossing

Kuo Chu Hwang, Nicholas J. Turro,\* and Charles Doubleday, Jr.\*

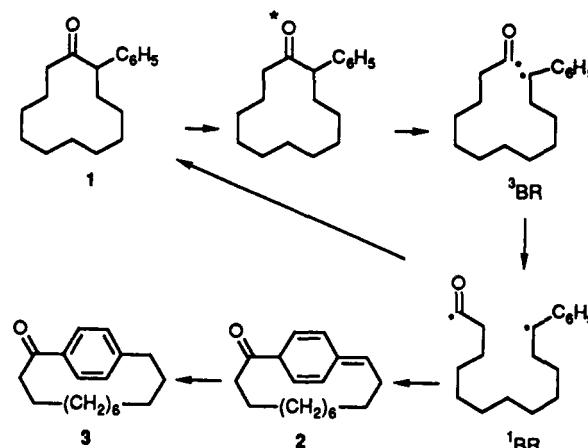
Contribution from the Department of Chemistry, Columbia University, New York, New York 10027. Received June 13, 1990

**Abstract:** In the absence of radical scavengers, the products of biradicals generated from photolysis of 2-phenylcycloalkanones exhibit no CIDNP. Addition of a radical scavenger such as  $\text{CCl}_4$  or  $\text{CBrCl}_3$  gives rise to strong CIDNP derived from  $\text{T}_0$ -S intersystem crossing. The CIDNP intensity depends on the scavenger concentration, the molecular chain length of the biradical, and the reaction temperature. The results are interpreted in terms of a simple kinetic scheme which implies a kinetic window within which  $\text{T}_0$ -S CIDNP is efficiently generated in biradicals. Bimolecular scavenging is sufficient to provide the strong competition with intersystem crossing needed to produce  $\text{T}_0$ -S CIDNP. From a knowledge of the dependence of CIDNP intensity on scavenger concentration and the previously measured biradical lifetimes, the rate constant of halogen atom abstraction by the acyl radical moiety is estimated to be  $1 \times 10^6 \text{ M}^{-1} \text{ s}^{-1}$  for Cl abstraction from  $\text{CCl}_4$  and  $1 \times 10^9 \text{ M}^{-1} \text{ s}^{-1}$  for Br abstraction from  $\text{CBrCl}_3$ .

#### Introduction

In radical pairs, CIDNP is usually generated by intersystem crossing (ISC) between the middle triplet level  $\text{T}_0$  and the singlet state S. Two things normally prevent  $\text{T}_0$ -S CIDNP from being observed in biradicals. First, biradicals have a significant singlet-triplet energy gap  $\Delta E_{\text{ST}}$  that arises from the radical centers being connected together so they cannot diffuse farther apart than the chain permits. If  $\Delta E_{\text{ST}}$  is much larger than the electron-nuclear hyperfine coupling (HFC),  $\text{T}_0$ -S ISC is inefficient and CIDNP is dominated by the interaction of S with one of the  $\text{T}_{\pm 1}$  levels, usually  $\text{T}_{-1}$ . Generally this means that  $\text{T}_0$ -S CIDNP is found only in long-chain biradicals, because  $\Delta E_{\text{ST}}$  decreases exponentially with increasing end-to-end distance in the biradical.<sup>1</sup> Second, even if  $\Delta E_{\text{ST}}$  is small enough, there must be a process competing with HFC which is independent of nuclear spin and leads to different products. If all mechanisms of biradical decay yield the same product distribution,  $\text{T}_0$ -S CIDNP cannot be produced because the total number of  $\alpha$  and  $\beta$  nuclear spins in the products is not changed by  $\text{T}_0$ -S ISC. In radical pairs the competing process is usually diffusive separation of the radicals.<sup>2</sup> Other possible competitive processes are spin-lattice relaxation,<sup>3a</sup> formation of triplet excited state products,<sup>3b</sup> spin-orbit coupling

Scheme I. Photoreaction of 2-Phenylcyclohexanone



in biradicals,<sup>3c,d</sup> and bimolecular radical scavenging of biradicals.<sup>4</sup> Kaptein showed that bimolecular scavenging of biradicals by radical scavengers can produce  $\text{T}_0$ -S CIDNP in the scavenging products, whose CIDNP resembles that of cage-escape products in ordinary radical pair CIDNP.<sup>4</sup> More recently, we have observed<sup>5</sup> that long-chain flexible biradicals generated from photolysis of 2-phenylcycloalkanones give no photo-CIDNP unless a bimolecular scavenging reaction provides a competition which allows  $\text{T}_0$ -S CIDNP to be generated. The maximum CIDNP signals are generated when the scavenging rate is comparable to the ISC rate.<sup>5</sup> This "kinetic window" for production of  $\text{T}_0$ -S CIDNP is

(4) DeKanter, F. J. J.; Kaptein, R. *Chem. Phys. Lett.* 1978, 58, 340.

(1) DeKanter, F. J. J.; denHollander, J.; Huizer, A.; Kaptein, R. *Mol. Phys.* 1977, 34, 857.

(2) (a) *Chemically Induced Magnetic Polarization*; Lepley, A. R., Closs, G. L., Eds.; Wiley and Sons: New York, 1973. (b) *Spin Polarization and Magnetic Effects in Radical Reactions*; Molin, Yu. N., Ed; Elsevier: Amsterdam, 1984.

(3) (a) Hutton, R. S.; Roth, H. D.; Kraeutler, B.; Cherry, W. R.; Turro, N. J. *J. Am. Chem. Soc.* 1979, 101, 2227. (b) Roth, H. D.; Manion-Schilling, M. L. *J. Am. Chem. Soc.* 1980, 102, 4303. (c) Doubleday, C., Jr. *Chem. Phys. Lett.* 1979, 64, 67; 1981, 79, 375. (d) DeKanter, F.; Kaptein, R. *J. Am. Chem. Soc.* 1982, 104, 4759.

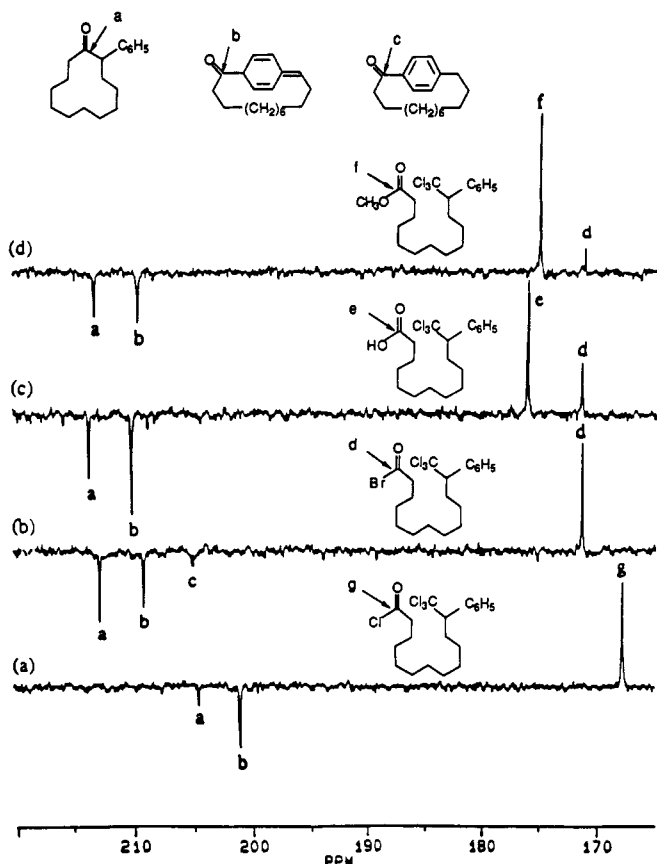


**Figure 1.**  $^{13}\text{C}$  CIDNP of 30 mM 2-phenylcyclododecanone (a) in  $\text{CCl}_4$  or in  $\text{CD}_3\text{CN}$  in the presence of (b) 10 mM  $\text{CBrCl}_3$  and in the presence of additional (c) 3% v/v  $\text{H}_2\text{O}$  or (d) 3% v/v methanol, measured on a Bruker AF 250 MHz ( $^1\text{H}$  frequency) FT NMR. The acquisition condition used is  $90^\circ$  rf pulse angle, 0.5-s acquisition delay time, and 1280 scans. No signals except the solvent (or methanol) peak were observed in all the dark spectra.

the subject of the current paper.

### Experimental Section

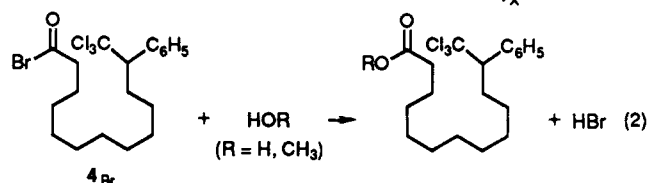
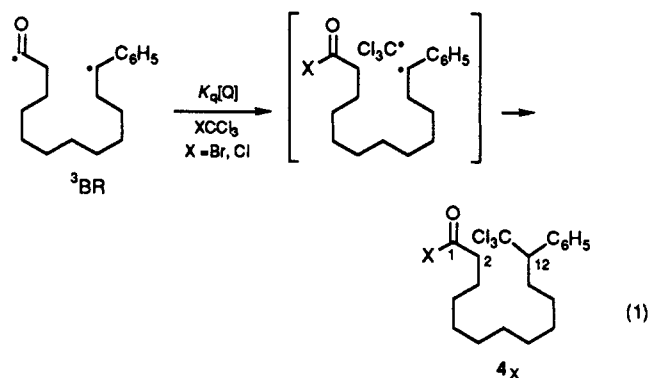
The syntheses and photochemistry of 2-phenylcycloalkanes were reported previously.<sup>6</sup>  $\text{CCl}_4$  (Aldrich Gold Label),  $\text{CBrCl}_3$  (Aldrich Gold Label), and  $\text{CD}_3\text{CN}$  (Aldrich, 99% D) were used as received. CIDNP measurements were performed on a Bruker AF 250 MHz FT NMR spectrometer with a modified probe<sup>5</sup> which allowed the introduction of UV light into the NMR chamber in the region of the detector coils. A 1000-W high-pressure Hg lamp with a  $\text{CoSO}_4$  aqueous filter solution was used as the light source. In  $\text{CCl}_4/\text{CD}_3\text{CN}$  solutions, the CIDNP intensities were normalized relative to the signal of benzene- $d_6$  which is in a capillary tube inserted into the NMR tube. In the  $\text{CBrCl}_3/\text{CD}_3\text{CN}$  solutions, all CIDNP intensities were measured and normalized relative to the  $\text{CD}_3\text{CN}$  solvent peak, since the amount of  $\text{CBrCl}_3$  added is less than 2% v/v. The CIDNP conditions for  $^1\text{H}$  CIDNP were a  $90^\circ$  rf pulse angle, 0-s time delay, and 2.7-s acquisition time. The conditions for  $^{13}\text{C}$  CIDNP were a  $90^\circ$  rf pulse angle, 0.5-s time delay, and 0.26-s acquisition time.

### Results

Photoexcitation of 2-phenylcyclododecanone (**1**, Scheme I) causes type I  $\alpha$  cleavage to generate triplet 1,12-acylbenzyl biradicals which, after ISC to the singlet state, collapse to regenerate **1** or to form a pre-cyclophane isomer **2** as major products.<sup>6</sup> **2** is stable for more than 5 h in acetonitrile at room temperature, but eventually it undergoes a proton shift to produce cyclophane **3**.

Figure 1 displays the observed  $^{13}\text{C}$  CIDNP in the carbonyl region at 250 MHz, produced by photolysis of **1** under various

conditions in the presence and absence of radical scavengers. The  $^{13}\text{C}$  CIDNP of 30 mM of **1** in acetonitrile is insignificant in argon-purged solutions in the absence of scavengers.<sup>5</sup> However, as seen in Figure 1a,b intense  $^{13}\text{C}$  CIDNP is developed by the addition of  $\text{CCl}_4$  (neat solvent) and  $\text{CBrCl}_3$  (10 mM in argon-purged acetonitrile), respectively. Spectra c and d in Figure 1 show that the inclusion of  $\text{H}_2\text{O}$  and  $\text{CH}_3\text{OH}$  causes significant changes in the high-field (170–180 ppm) regions but not in the low-field (205–215 ppm) regions of the carbonyl portion of the spectrum. The enhanced emissions a, b, and c in Figure 1 at 212, 209, and 205 ppm, respectively, are assigned to the carbonyl carbons of the cyclanones **1**, **2**, and **3**, respectively, based on comparison with authentic samples. The enhanced absorptions (d and g) at 171 and 168 ppm are respectively assigned to the carbonyl carbon of **4<sub>Br</sub>** and **4<sub>Cl</sub>**, presumably involved in the following reactions.



As can be seen from Figure 1c,d, in the presence of a small amount of  $\text{H}_2\text{O}$  (or  $\text{CH}_3\text{OH}$ ) the intensity of the peak at 171 ppm decreases and a new enhanced absorption band at 176 ppm (or 175 ppm) appears and corresponds to the carbonyl carbon of the acid (or ester) derived from the reaction of **4<sub>Br</sub>** with  $\text{H}_2\text{O}$  (or  $\text{CH}_3\text{OH}$ ). The results clearly indicate that the rate of hydrolysis (or esterification) of **4<sub>Br</sub>** is very fast. These observations provide further support for the structure of **4<sub>Br</sub>**, and are also consistent with the previous observation that the halogen atom abstraction by the acyl radical center is the first step in reaction of acyl benzyl biradicals with tetrahalomethanes.<sup>5</sup>

**Dependence of Quencher Concentration.** The  $^{13}\text{C}$  CIDNP intensities from the carbonyl carbons of **1**, **2**, and **4<sub>Br</sub>** (or **4<sub>Cl</sub>**) was studied as a function of the scavenger concentration in acetonitrile and are shown in Figure 2. The scavengers used are  $\text{CCl}_4$  and  $\text{CBrCl}_3$ . In the case of  $\text{CCl}_4$  (Figure 2a) the CIDNP intensities were compared to the signal of benzene- $d_6$  standard. In the case of  $\text{CBrCl}_3$  (Figure 2b) the CIDNP intensities were measured relative to the  $\text{CD}_3\text{CN}$  solvent intensity (the amount of  $\text{CBrCl}_3$  added was less than 2% v/v). Increasing the  $\text{CCl}_4$  concentration from 2 to 10.3 M (neat solution) causes stronger polarization in all carbonyl carbons of **1**, **2**, and **4<sub>Cl</sub>**. In the case of  $\text{CBrCl}_3$  (Figure 2b), the CIDNP polarization shows a maximum at ca. 10–20 mM  $\text{CBrCl}_3$ . In neat  $\text{CBrCl}_3$ , no CIDNP could be observed.

**Biradical Chain Length.** The CIDNP intensities were studied as a function of biradical chain length starting from cyclic ketones **1<sub>n</sub>** with  $n = 9\text{--}12, 15$ . All 2-phenylcycloalkanes used in this study show significant CIDNP only when in the presence of radical scavengers. The solutions of 2-phenylcycloalkanes in  $\text{CCl}_4$  were purged with argon for 15 min before irradiation. A capillary tube containing benzene- $d_6$  was inserted into the sample tube to lock the NMR signal. All polarization intensities were measured by comparison with the  $\text{CCl}_4$  solvent intensity. As shown in Figure 3, the polarization intensities of carbonyl carbons of **1**, **2**, and **4<sub>Cl</sub>**

(5) Hwang, K. C.; Rao, P. V.; Turro, N. J.; Doubleday, C. J. *Phys. Chem.* In press.

(6) Lei, X. G.; Doubleday, C.; Turro, N. J. *Tetrahedron Lett.* **1986**, 27, 4671, 4675.

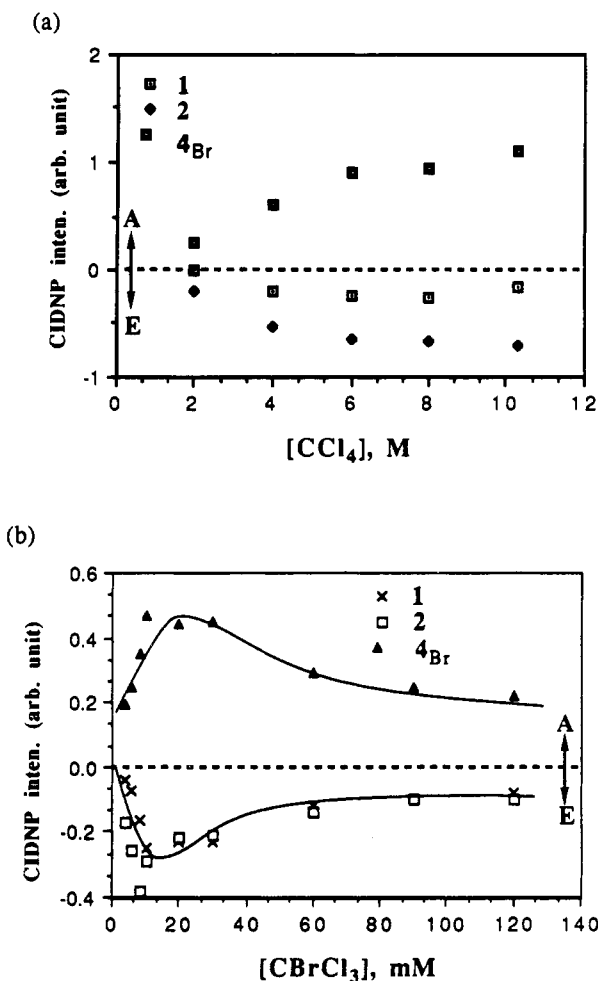


**Figure 2.**  $^{13}C$  CIDNP intensities from irradiation of 30 mM 2-phenylcycloalkanone in acetonitrile were measured at 25 °C (a) as a function of  $CCl_4$  concentration with CIDNP intensities measured relative to a benzene external standard and (b) as a function of  $CBrCl_3$  concentration with CIDNP intensities measured relative to the acetonitrile solvent intensity, since the amount of  $CBrCl_3$  added is less than 2% v/v relative to the solvent (A, enhanced absorption; E, emission).

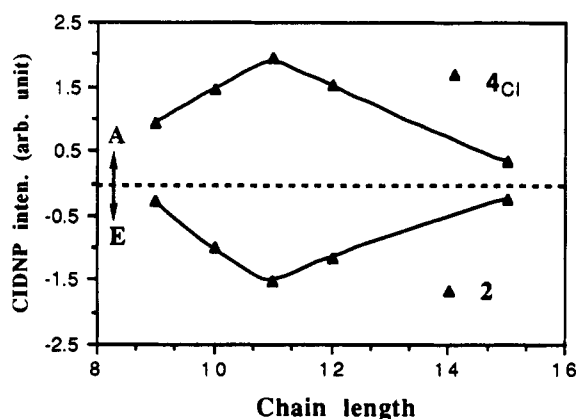


**Figure 3.**  $^{13}C$  CIDNP intensities from irradiation of 30 mM 2-phenylcycloalkanone in neat  $CCl_4$  were measured as a function of molecular chain length (chain length  $n = 9, 10, 11, 12,$  and  $15$ ) at 25 °C (A, enhanced absorption; E, emission). A capillary containing benzene- $d_6$  was inserted into the NMR tube to lock the NMR radio frequency. The intensities were measured relative to the  $CCl_4$  solvent intensity.

show the same trend: the CIDNP intensities increase from  $n = 9, 10,$  to  $11$  and then drop from  $n = 11, 12$  to  $15$ .

**Temperature-Dependent CIDNP.** The CIDNP of 30 mM 2-phenylcycloalkanone in  $CCl_4$  was studied as a function of temperature (Figure 4). The CIDNP intensities were measured

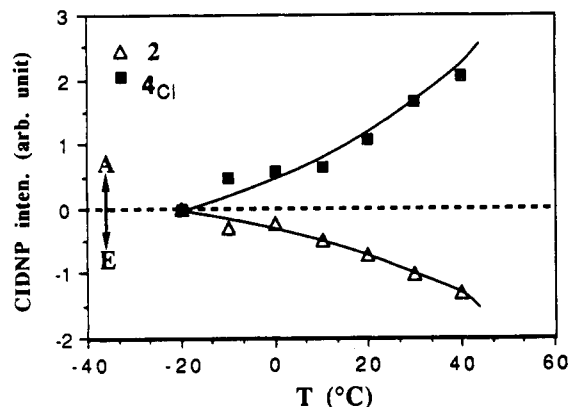
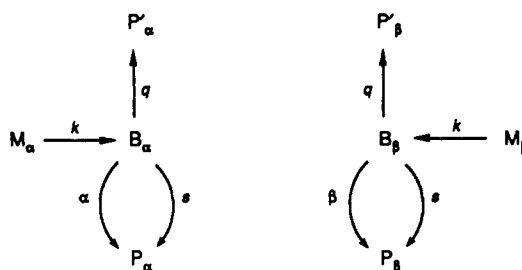


**Figure 4.**  $^{13}C$  CIDNP intensities from irradiation of 30 mM 2-phenylcycloalkanone in neat  $CCl_4$  were measured as a function of temperature (A, enhanced absorption; E, emission). The intensities were measured relative to the  $CCl_4$  solvent intensity.

**Scheme II.** Postulated Pathways for a Qualitative Understanding of the "Kinetic Window" Concept for Generating  $T_0$ -S CIDNP



relative to the solvent intensity. The trends of the CIDNP intensities of carbonyl carbons of 1, 2, and 4Cl are the same: they decrease at lower temperatures.

### Discussion

To get a qualitative understanding of the kinetic window within which  $T_0$ -S CIDNP can be generated, we consider Scheme II. This is the simplest possible scheme for discussing the effect of scavenging on CIDNP.<sup>7</sup> Scheme II shows a pair of decoupled reactions, one for  $\alpha$  and one for  $\beta$  nuclear spin. In each case, starting material  $M$  produces an intermediate triplet biradical  $B$ , which then partitions between the intramolecular product  $P$  and the bimolecular quenching product  $P'$ . Rate constants  $q$  and  $s$  are respectively the pseudo-first-order quenching rate constant (containing quencher concentration) and nuclear spin independent ISC (e.g., ISC occurs through spin-orbit coupling, SOC). Rate constants  $\alpha$  and  $\beta$  refer to ISC involving nuclear spins  $\alpha$  and  $\beta$  and involve the usual CIDNP spin Hamiltonian terms  $\Delta g\beta H$  and the HFC constants. The ISC processes  $s, \alpha,$  and  $\beta$  all proceed via an intermediate singlet biradical, which is not shown because ISC is rate determining at room temperature and above.<sup>8</sup>

For simplicity let the initial amounts of  $M_\alpha$  and  $M_\beta$  be equal at time  $t = 0$ :  $M_\alpha^0 = M_\beta^0 = 1/2$ . At  $t = \infty$  stoichiometry requires  $M_\alpha^0 = P_\alpha + P'_\alpha$  and  $M_\beta^0 = P_\beta + P'_\beta$ . The polarization is defined as  $P_\alpha - P_\beta$  and  $P'_\alpha - P'_\beta$  for products  $P$  and  $P'$ , respectively, and the symmetry of the reaction scheme demands  $P_\alpha - P_\beta = -(P'_\alpha - P'_\beta)$ . From Scheme II the fraction of  $P_\alpha$  derived from  $M_\alpha^0$  is  $(\alpha + s)/(\alpha + s + q)$ . With neglect of nuclear relaxation this gives

$$P_\alpha - P_\beta = \frac{1}{2} \left( \frac{\alpha + s}{\alpha + s + q} - \frac{\beta + s}{\beta + s + q} \right) = \frac{q}{2} \frac{\alpha - \beta}{(\alpha + s + q)(\beta + s + q)}$$

(7) Chain motions are included implicitly via the SOC rate constants. CIDNP is generated mainly in biradical conformers with large end-to-end distances. Scheme II then corresponds to a high-temperature approximation for the chain dynamics.

(8) Doubleday, C., Jr.; Turro, N. J.; Wang, J.-F. *Acc. Chem. Res.* **1989**, *22*, 199.

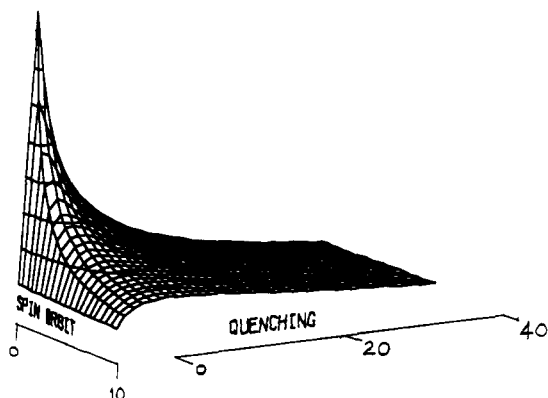


**Figure 5.** Relative CIDNP intensity (arbitrary units) vs dimensionless SOC and bimolecular quenching represented by  $s'$  and  $q'$ , respectively, calculated from eq 3 with  $d' = 0.25$ .

To avoid working with absolute rate constants we first define the average and difference rate constants  $a = (\alpha + \beta)/2$  and  $d = (\alpha - \beta)/2$  so that  $\alpha = a + d$  and  $\beta = a - d$  and then work with the dimensionless parameters  $d' = d/a$ ,  $s' = s/a$ , and  $q' = q/a$ . The  $d'$  parameter then depends only on the  $T_0$ -S matrix elements, which are known. In terms of  $d'$ ,  $s'$ , and  $q'$  the polarization is

$$P_\alpha - P_\beta = \frac{d'q'}{(1 + d' + s' + q')(1 - d' + s' + q')} \quad (3)$$

The maximum polarization occurs when  $q' = [(s' + 1)^2 - d'^2]^{1/2}$  or  $q' = [(\alpha + s)(\beta + s)]^{1/2}$ , i.e., when the quenching rate constant is equal to the geometric mean ISC rate constant.

Equation 3 contains two adjustable parameters,  $s'$  and  $q'$ , since  $d'$  can be calculated from ESR data. The  $T_0$ -S matrix element  $A/4 = 91$  MHz, where  $A$  is the  $^{13}\text{C}$  HFC constant of 130 G. In our 58.3-kG magnet the  $T_0$ -S matrix element  $\Delta g\beta H/2 = 156$  MHz. Assuming the ISC rate constant varies as the square of the matrix element, we have  $a \propto 156^2 + 91^2$  and  $d \propto 91^2$ , which gives  $d' = 91^2/(156^2 + 91^2) = 0.25$ . With this value of  $d'$ , Figure 5 shows the polarization surface as a function of  $s'$  and  $q'$ , the reduced SOC and quenching rate constants.

The most obvious feature is that the kinetic window is narrower when SOC is small and broader when SOC is large compared to HFC. Our previous work on these acylbenzyl biradicals suggested that  $s' \approx 6-7$ .<sup>9</sup> Figure 5 then implies a wide kinetic window, or range of quencher concentrations, within which  $T_0$ -S CIDNP can be observed. Another feature of Figure 5 is that the maximum CIDNP intensity moves to larger values of  $q'$  as SOC gets larger, in accord with the requirement that the quenching rate match the geometric mean ISC rate.

Regardless of SOC, Figure 5 implies that the bimolecular scavenging rate constant can be deduced if the biradical lifetime is known and if ISC is the rate-limiting step for biradical decay (e.g., room temperature or above in fluid solution). The maximum in a plot of CIDNP vs quencher concentration corresponds to a match between quenching and ISC, so the quenching rate constant is just  $(\tau[Q_{\text{max}}])^{-1}$ , where  $\tau$  is the biradical lifetime and  $[Q_{\text{max}}]$  is the quencher concentration that produces the maximum CIDNP

intensity. Figure 2b shows such a maximum, and we obtain  $k_Q = [(73 \text{ ns})(0.015 \text{ M})]^{-1} \approx 1 \times 10^9 \text{ M}^{-1} \text{ s}^{-1}$  for abstraction of Br from  $\text{BrCCl}_3$  by the acyl radical moiety. This is a simple method of obtaining a rate constant which is difficult to obtain directly because of the lack of an easily detectable chromophore. Figure 2a shows no clear maximum, but it may be approaching a maximum at 10.3 M  $\text{CCl}_4$ . If so, it implies a rate constant for Cl abstraction 3 orders of magnitude slower than Br abstraction.<sup>11</sup>

Equation 3 also exhibits a maximum when plotted as a function of  $d'$ , the difference in ISC rates for  $\alpha$  and  $\beta$  nuclear spins. This can be realized experimentally by varying the biradical chain length  $n$  as in Figure 3. The average end-to-end distance  $R$  of the biradical chain increases with increasing  $n$ . The effective value of  $\Delta E_{\text{ST}}$  decreases approximately exponentially as  $R$  increases,<sup>1</sup> and the ISC rate constant is observed to increase<sup>8</sup> with increasing  $n$  because the  $T_0$  and S states get closer together. The abscissa of Figure 3 is basically  $\log d'$ , since in the range of  $n$  considered here  $R$  increases approximately linearly with each incremental  $\text{CH}_2$  group.<sup>10</sup> A plot of CIDNP intensity vs  $\log d'$  based on eq 3 strongly resembles Figure 3, though the uncertainties in the parameters preclude a fit. The maximum in Figure 3 can be interpreted in the same way as the maximum in Figure 2b. With 10.3 M  $\text{CCl}_4$  and  $\tau = 65 \text{ ns}$  we estimate  $k_Q = 1.5 \times 10^6 \text{ M}^{-1} \text{ s}^{-1}$ , close to our estimate from Figure 2a.

The temperature dependence shown in Figure 4 contains several complex processes, including the temperature dependence of ISC, scavenging, and spin-lattice relaxation. However, the overriding effect is probably that ISC ceases to be the rate-determining step for biradical decay below about  $-20^\circ\text{C}$ .<sup>8</sup> Below this temperature chain motions become rate limiting, singlet and triplet states have time to equilibrate, and CIDNP goes to zero. The temperature dependence of bimolecular scavenging works in the same direction. Thus the qualitative behavior is obvious a priori, although the exact shape of the curve depends on several effects.

## Conclusions

Competition between bimolecular scavenging and ISC gives rise to a kinetic window within which steady-state  $T_0$ -S CIDNP is maximal. The general condition for maximum CIDNP intensity is that the scavenging rate match the geometric mean ISC rate. These effects were investigated by measuring CIDNP as a function of scavenger concentration, biradical chain length, and temperature. This report also demonstrates the potential of using ISC as an internal clock to measure the rate of bimolecular scavenging, or vice versa. By this method the rate constant of halogen atom abstraction by the acyl radical moiety of acyl-benzyl biradicals is estimated to be  $1 \times 10^6 \text{ M}^{-1} \text{ s}^{-1}$  for abstracting Cl from  $\text{CCl}_4$  and  $1 \times 10^9 \text{ M}^{-1} \text{ s}^{-1}$  for abstracting Br from  $\text{CBrCl}_3$ .

**Acknowledgment.** K.C.H. and N.J.T. thank the Air Force Office of Scientific Research, the National Science Foundation, and the Department of Energy for their generous support of this research. C.D. gratefully acknowledges NSF Grant CHE-8721164 for support and the Pittsburgh Supercomputing Center for assistance with the graphics. K.C.H. thanks Mr. X. G. Lei for collaboration in developing the synthesis of the 2-phenylcycloalkanones.

(10) Schulten, K.; Bittl, R. *J. Chem. Phys.* **1986**, *84*, 5155.

(11) The rate constants for halogen atom abstraction by the acyl portion of an acyl-benzyl biradical will be described in detail in another manuscript: Jenks, W.; Hwang, K. C.; Turro, N. J. Manuscript in preparation.

(9) Zimmt, M.; Doubleday, C.; Turro, N. J. *J. Am. Chem. Soc.* **1985**, *107*, 6726.